TRABAJO INVITADO

Runaway stars: their impact on the intestellar medium

P. Benaglia[1,2], I. R. Stevens[3], C. S. Peri[1,2]

(1) Instituto Argentino de Radioastronomía, CCT-La Plata, CONICET
(2) Facultad de Ciencias Astronómicas y Geofísicas, Universidad Nacional de La Plata
(3) School of Physics and Astronomy, University of Birmingham, Edgbaston, Birmingham, B15 2TT, UK

Abstract. Runaway, massive stars are not among the most numerous. However, the bow shocks built by their supersonic movement in the interstellar medium have been detected in the infrared range in many cases. Most recently, the stellar bow shocks have been proposed as particle acceleration sites, as radio data analysis at high angular resolution have shown. We present results of different manifestations of the stellar bow-shock phenomenon, revealed from modern IR databases.

Resumen. Las estrellas masivas fugitivas no son de las más numerosas. Sin embargo, los *bowshocks* formados debido a su movimiento supersónico en el medio interestelar han sido detectados en el rango infrarrojo en muchos casos. Muy recientemente, estos *bowshocks* estelares fueron propuestos como sitios de aceleración de partículas, como lo sugiere el análisis de datos de alta resolución angular a bajas frecuencias de radio. Se presentan aquí resultados de distintas manifestaciones relacionadas con *bowshocks* estelares, revelados a partir de las bases de datos IR más modernas.

1. Runaway stars

The seminal studies on stars with high velocities ($v_* \gtrsim$ tens of km s^{-1}) were carried out during the '50s by A. Blaauw and collaborators. Among other findings, they pointed out that an important number of early-type stars (O-B5) move faster than the surrounding objects. The motion of some of them could be interpreted as if the stars are escaping from their parental associations: see Blaauw & Morgan (1954) and the case of the stars AE Aur and μ Col. The name 'runaway stars' was thus coined by Blaauw (1961), who, together with Zwicky (1957), suggested that the velocity kick could be given by a supernova companion in an originally binary system. In those first studies, the velocity distribution of OB stars with v_* up to $\sim$ 30 km s^{-1} was reasonable fitted by a gaussian, but an important number of stars with greater velocities failed the fit. After compiling proper motion information of O stars up to 2 kpc, Stone (1979) concluded that there were two stellar populations: one of low spatial velocities (below 25 km s^{-1}) and the rest with higher velocities (see Figure 1). He fitted

both velocity distributions with gaussian functions. Very recently, Tetzlaff et al. (2010) carried out a comprehensive study on Hipparcos stars, and built a catalogue of runaway stars. Following former ideas, the authors fit spatial velocity distributions to the catalogued objects[1].
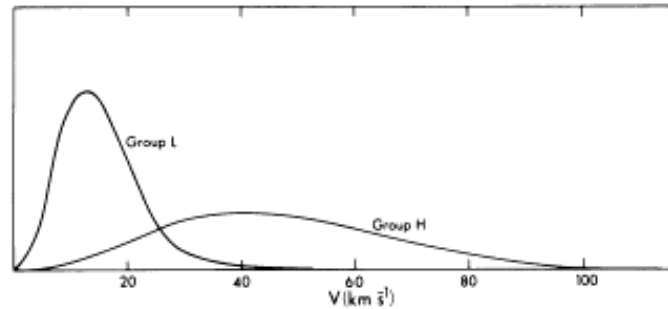

Figure 1.   Velocity frequency functions for the two groups of O stars up to 2 kpc; L: low velocity stars, H: high velocity stars (Stone 1979).

The input sample of Tetzlaff et al. (2010) consisted of a database of thousands of stars up to 3 kpc from the Sun. By computing runaway star probabilities, the authors catalogued a 27% of runaways throughout the sample. The importance of this study lies on the extent and uniformity of the sample, which is not biased by spectral type or visual magnitude, like previous ones.

Conclusive evidences that at least two different mechanisms operate in nature to 'kick' a star have been presented (e.g., Hoogerwerf et al. 2000). The processes are referred as the Binary Supernova Scenario (BSS) and the Dynamical Ejection Scenario (DES). In the last years, extensive N-body simulations have been carried out, that could explain the observed ejection rate solely by the action of close gravitational encounters (see Perets & Subr 2013 and references therein). The knowledge of the exact multiplicity status of the runaway star is crucial to test its origin[2]. More realistic results will be obtained as long as forthcoming instruments allow deeper studies.

Runaway stars can be used as tools to trace galactic structure. Silva & Napiwotzki (2013) have shown, with a local sample of high-latitude runaway stars, that an analysis of the birthplaces help to map the spiral arms and determine galactic dynamics. The method will be terribly powerful when instruments like *Gaia* come to play.

-----

[1] We will not consider here the so-called *hypervelocity stars*, which are originated in three-body encounters that include a high mass black hole as the Galactic center one.

[2] As Virpi Niemela likes to say: "with evidence at hand, it is ussually straightforward to state that a star is a binary, but it is more than difficult to ensure that is single".

2. Stellar bow shocks: theory and observations

A star moving through a slower interstellar medium will form a thin layer of swept-up gas. An early-type star, that has developed strong stellar winds (OB or Wolf-Rayet star) will stack matter on a thicker layer.

If the stellar motion is supersonic with respect to the ambient gas velocity, shock waves are produced. A discontinuity surface is formed, and two shock fronts in opposite directions. A 'forward' shock in the direction of the stellar motion travels with a velocity similar to the stellar velocity. A 'reverse' shock from the discontinuity to the star has a velocity of the order of the stellar wind terminal velocity, which can be, in some cases, a few thousands of km s^{-1}. In Figure 2 we show a simplified scheme of the situation. The width of the discontinuity will depend on the cooling process: adiabatic, radiative or a mixed case. Ideally, four regions can be identified: the closer to the star with free wind, that of shocked wind (where the reverse shocked has passed), the shocked ambient matter region and the not-yet-disturbed ISM region.
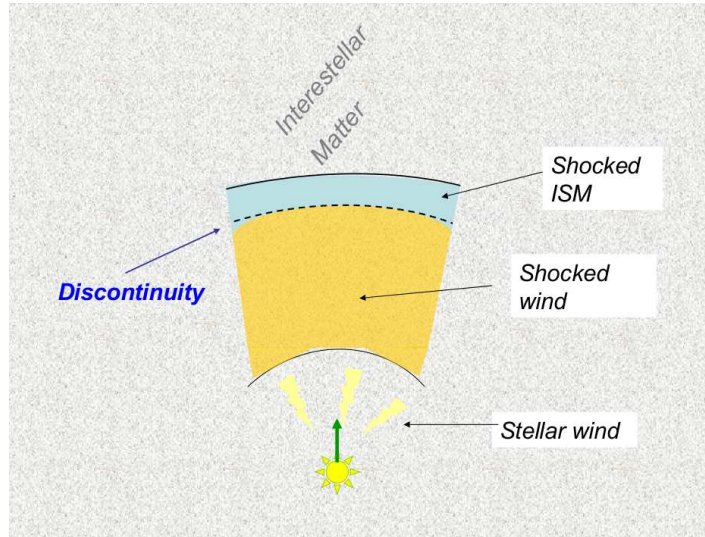

Figure 2.   Scheme of a stellar bow shock generated by a star with supersonic motion related to the ambient media. The different regimes are shown. The green vector represents the stellar velocity.

The matter surrounding the stars is piled-up in a feature that resembles the sea foam which is pushed by the bow of a ship, from where the stellar bow shock takes its name. For the faster stars, it resembles a cometary tail.

The arc-shaped structure moves in the same direction of the stellar velocity vector. The stellar winds are confined by the ISM pressure. The point where the momentum of the wind balances that of the ISM is defined as the stagnation point R_0.

The shocked ISM heats the swept-up matter, and the dust re-radiates strongly as an excess at MID and FIR wavelengths. Consequently, stellar bow shocks of massive, early type stars are revealed at infrared frequencies. In Figure 3 we present the infrared emission from a stellar bow shock produced by the run-

away star HD 77581, better known as Vela-X1, a HMXB formed by a B0.5 Iae star (Prinja & Massa 2010) and a compact object. The IR images are part of the Wide-field Infrared Survey Explorer (WISE, Wright et al. 2010). The structure is detected at the observed bands 1 to 4 (respectively centred at 3.4, 4.6, 12, and 22 μm). Since the heat can be enough to ionise the gas, some bow shocks are also seen at the Hα emission line (like this one, Kaper et al. 1997) and radio continuum. The dust contains policyclic aromatic hydrocarbons (PAHs) with emission features at some WISE bands (1 and 3). The features are excited by non- ionizing UV photons from the stellar radiation field and the dust becomes bright. The stellar UV field also ionizes the interstellar gas, which de-excites via recombination lines like Brα (WISE band 2). The WISE band 4 is sensitive to emission from warm dust.

From the IR images it is possible to derive the density of the ISM, by measuring the distance from the star to the shock, once the stellar velocity, the mass loss rate and the wind terminal velocity are known.
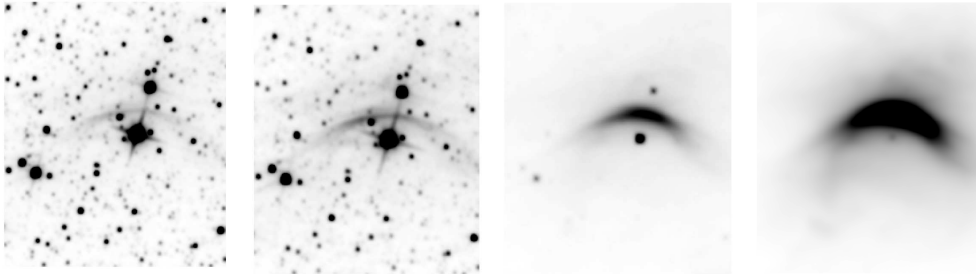

Figure 3.   Field of HD 77581 (Vela-X1): emission in WISE bands 1 (3.4 μm), 2 (4.6 μm), 3 (12μm) and 4 (22 μm), from left to right. The bow shock feature and the star HD 77581 are seen at all bands. The star can be better identified at band 3, close to the bow shock and to the south.

There is much theoretical work carried out on bow shock dynamics (see references in Peri et al. 2012, and del Valle and Romero 2012, for instance). The first attempts considered 1-D modelling, a thin-shell, uniform density. Gradually, they included density gradients, misaligned winds, slow and fast winds, fluid instabilities, clumped winds, (non-uniform) magnetic fields, rotating flows, etc. To cite a few, Gustafsson et al. (2010) built 3D models of interstellar bow shocks propagating in a homogeneous molecular medium with a uniform magnetid field. The authors found that the bow shock shape depends strongly on the orientation of the magnetic field, and could reproduce H$_2$ emission lines detected from the bow shock of the source OMC1.

Cox et al. (2012) carried out 2D hydrodynamical simulations of interactions between the ISM and the circumstellar medium to analyze how the morphology of the bow shock varies with stellar wind and ISM parameters. They used a model to describe bow shocks around AGB stars as seen by data obtained with the Herschel space telescope.

Acreman, Stevens and Harries (2013) made use of hydrodynamical modelling and Monte-Carlo radiative transfer calculations to find the radiation influenced region around a runaway early-type star. The authors generated IR,

Hα and radio observables and obtained a good match between synthetic and real images.

Despite detailed studies on individual 'famous' stars with bow shocks, or clusters rich in early-type stars (i.e. Vela X-1: Kaper et al. 1997; Cyg OB2: Kobulnicky et al. 2010; BD+43° 3654: Comerón & Pasquali 1998, to quote a few), one can still ask basic questions like in which scenarios (ISM and star) a bow shock is formed, how it evolves or under which conditions it is detected. A crucial issue is how observations fill in theoretical developments or, more precisely, how models fit the data? Undoubtely, the study of a large-enough sample of such objects will bring the answers closer, and allow to perform real statistics.

3.   Stellar bow shock surveys

After the outstanding view of the sky by the IRAS satellite, Noriega-Crespo et al. (1997) analized the infrared emission from the surrounding field of about 60 early-type stars. The angular resolution of the data was $\sim 1'$. The emission was classified as diffuse, bubble- or bow-shock like. The authors presented results of around 20 stellar bow shock candidates among the total sample.

Following IR space telescopes improved the data angular resolution, like the case of the Midcourse Space eXperiment (MSX, $18''$, Egan et al. 2003). The IRAS (all-sky covering) successor was the Wide-field Infrared Survey Explorer[3]. WISE observing bands resolutions were 6.1, 6.4, 6.5, $12''$ respectively. The sensitivity resulted in hundreds of times better than that of IRAS. The telescope was active from December 2009 to February 2011. In early 2011 the WISE team published a first data release encompassing observations towards 57% of the sky.

At the same time, a large database of runaway stars was made publicly available: the catalogue of young runaway Hipparcos stars within 3 kpc from the Sun already mentioned (Tetzlaff et al. 2010). From an initial sample of 7663 stars, the authors compiled information on proper motions, parallaxes, spectral types, radial velocities and estimate distances, ages, spatial velocites, and aggregate membership. After a probabilistic study, by means of mainly computed velocities, they converged on a catalogue of runaway stars candidates of about 2400 objects.

Taking into account two kinds of samples, the one of Noriega-Crespo et al. (1997), and the Tetzlaff et al. (2011) catalogue, Peri et al. (2012) conducted a systematic search of stellar bow shocks. The first list had already detected IR stellar bow shocks, so the main goal was to compare IRAS data with WISE data. In many cases the classification of stellar bow shock remained, and also new bow shocks were discovered. For the second sample, the authors seeked to test the theoretical assumption that the runaway stars generate observable stellar bows shocks. For the first list, that of Noriega-Crespo et al., they found 14 of the IRAS bow shocks in WISE, and 4 more mixed, through WISE and MSX data; the rest had no new IR data, or no bow shock. For the second

---

[3]Funded by NASA; contributing institutions: UCLA, JPL, IPAC/Caltech, UC Berkeley, SDL, BATC.

sample (only stars of spectral types from O to B2, in total 244), they found 17 bow shocks, 80 objects with no data on WISE, and 147 with no bow shock. Results on the first list confirm the already observed bow shocks, and brought some new examples. Those of the second list showed that about a 10% of the sources had an associated bow shocks. But probably the most important result was the confirmation that the stellar bow shocks can form ot not, anf if they form they can have different structures. This conclusion can be analized looking at the IR images and the several parameters that caracterize all the stellar bow shocks candidates. This issue has been studied through numerical simulations by Comerón and Kaper (1998) and seems so far that the observations correlate with the existing models very well.

E-BOSS bow shocks are depicted in Figure 4. On March 2012 the WISE team published IR images and data of the remaining sky (43%). The second version of E-BOSS is under way, and it will include results on the search at the WISE second release database.

4.   Bow shocks as particle acceleration regions

Nearby windy stars with supersonic motion relative to the ISM, particles can be accelerated up to relativistic velocities via first order Fermi mechanism by repeatedly crossing the discontinuity surface (Bell 1978). It can be demonstrated that protons easily diffuse towards the 'tail' of the bow shock, but that is not the case for the -less-massive- electrons.

The shock wave compresses the gas. The magnetic field is coupled with the gas, and increases its energy density. Consequently, the magnetic field is much amplified at the post-shock region, where the shock wave is stronger ($\propto$ wind terminal velocity) (e.g. Longair 1997). The interaction of the relativistic electrons with the post-shock B field will give rise to synchrotron radiation, detectable at radio wavelengths. In Figure 5 we represent the scenario: the ISM magnetic field B_{ISM}, the amplified field at the post-shocked region (B'), the electrons gaining energy by crossing the discontinuity surface, and the protons diffusing outwardly.

To look for signatures of synchrotron emission we carried out radio interferometric observations toward the field of the O4 supergiant BD +43° 3654 (Benaglia et al. 2010). Comerón & Pasquali (2007) had proposed that this is a runaway star from the Cyg OB2 association, and found a bow shock feature at MSX images. The radio data were taken at two bands: 1.4 and 4.8 GHz, and the bow shock was detected at both of them. A spectral index map and its corresponding error map were then built (see Figure 6). The average value of the spectral index resulted in ~ -0.4, consistent with non-thermal emission. Conclusive evidence of pure synchrotron emission will confirm the presence of a relativistic electrons population. These particles will also be involved in high energy processes.

Later observations with the Giant Metrewave Radio Telescope at 0.61 and 1.25 GHz by Brookes et al. (2013) confirmed the former results.

If the radio emission is mainly produced by synchrotron processes, one can use the measured radio flux and spectral index as input for a model of the SED. Del Valle & Romero (2012) showed that the bow shock of a star like ζ Oph,
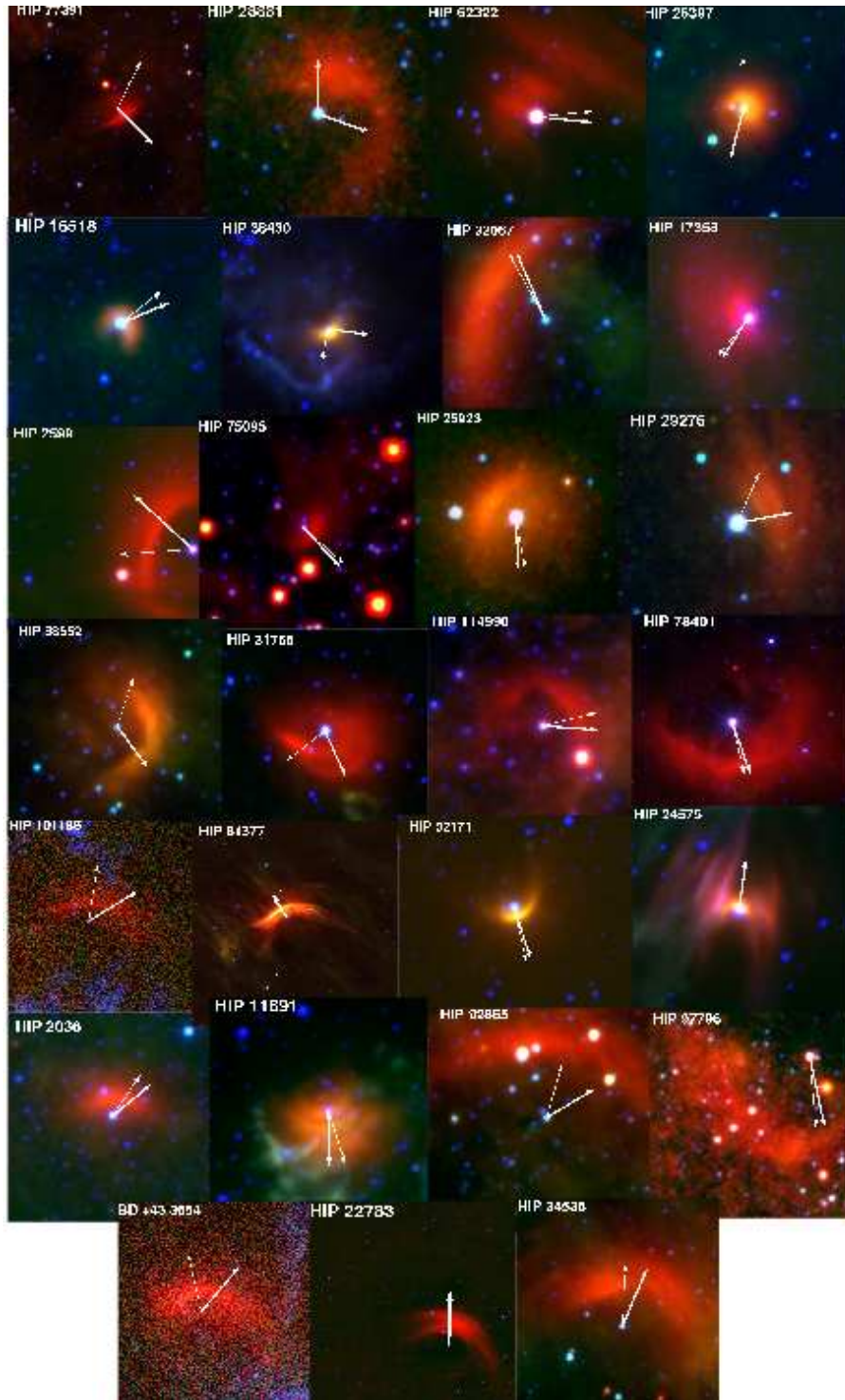
Figure 4. WISE images of the E-BOSS.v1 members (Peri et al. 2012). Vectors: proper motions from Hipparcos (thicker) and corrected for the ISM Galactic rotation. The star name is given in the top right corner.
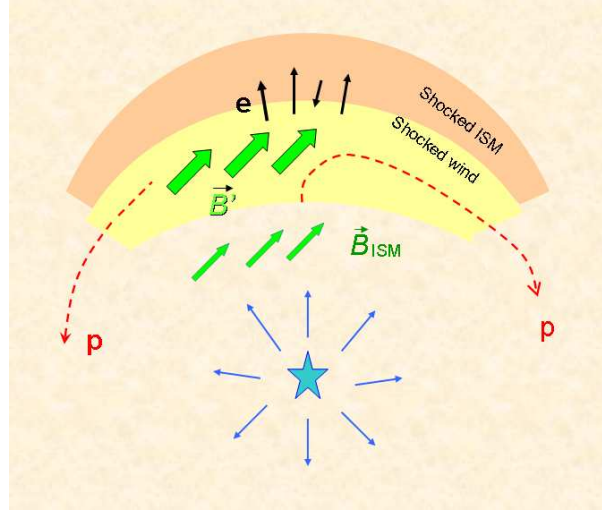
Figure 5.   Regions of particle acceleration up to relativistic energies: the
star (in blue), the free stellar wind (blue arrows); the shocked wind region
(light yellow), the shocked ISM region (pale orange). 'p' is for protons, and
'e' for electrons. The interstellar magnetic field $\mathbf{B}_{ISM}$ is represented by the
smaller green arrows. This magnetic field is amplified at the post-shocked
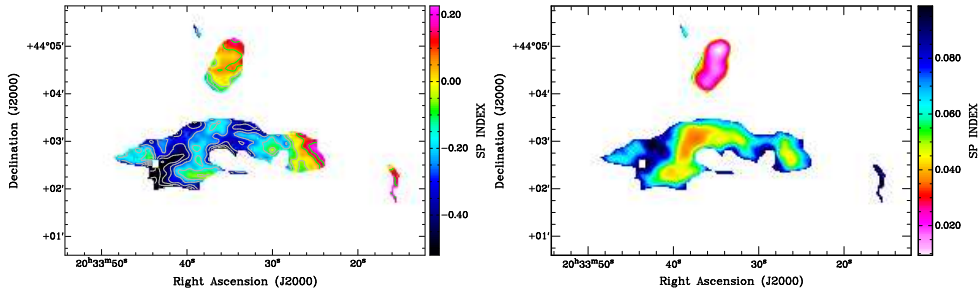region, as $\mathbf{B}'$.

Figure 6.   Spectral index map and spectral index error map of the radio
emission associated with the stellar bow shock of BD+43^{0}3654 (see Benaglia
et al. 2010).

detected at WISE bands, could produce, under certain conditions, high energy
emission measurable by forthcoming instruments like the Cerenkov Telescope
Array (see Figure 7).

    Another way to look for non-thermal emission is by means of X-ray data
analysis. Lopez-Santiago et al. (2012) studied the fields of the E-BOSS candi-
dates through XMM-Newton observations. They detected the star HIP 24575
(AE Aur), but also an XMM source, BS, on the position of the bow shock (see
Figure 8). They showed that the BS emission could be fitted by a non-thermal
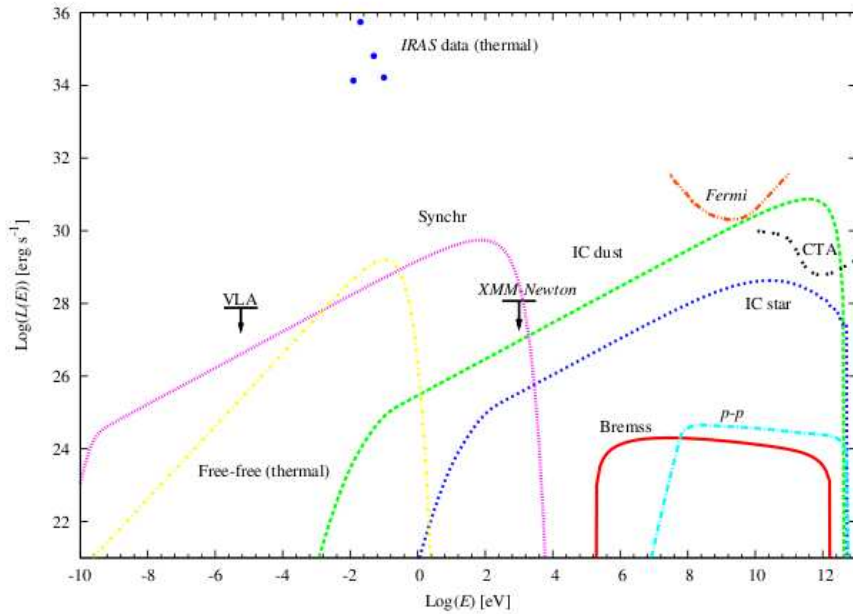component.

Figure 7.   Spectral energy distribution of ζ Oph (see del Valle & Romero 2012). Various mechanisms for high energy production have been modelled.
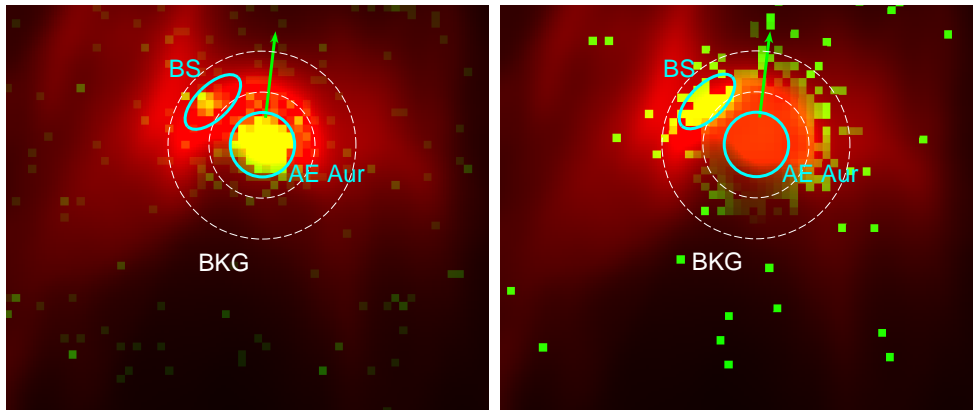

Figure 8.   In red: WISE 12.1μm image. In yellow: XMM-Newton EPIC emission in the keV bands $1 - 8$ (right), and $0.3 - 8$ (left).

5.   Further studies

Detailed studies on stellar bow shocks, either planned or under way, include the followings:

- Carry out bow shock searches around stars with spectral types different from O-B2;
- Perform statistics over the full (final) bow shock candidate catalogue;

- Improve 3D modelling adding magnetohydrodynamics, thermal radio emission, and wind and ISM inhomogeneities;

- Implement dedicated observations toward the bow shocks with signs of non-thermal radio emission;

- Look for polarised radio emission from bow shocks to confirm synchrotron origin.

References

Acreman, D.M., Stevens, I.R., Harries, T.J. 2013, in press

Bell, A.R. 1978, MNRAS 182, 443

Benaglia, P., Romero, G.E., Martí, J., Peri, C.S., Araudo, A.T. 2010, A&A, 517, L10

Blaauw, A. & Morgan 1954, ApJ, 119, 625

Blauuw, A. 1961, BAN, 15, 265

Brookes, D., et al. 2013, in preparation

López-Santiago, J., Micheli, M., del Valle, M.V., et al. 2012, ApJ, 757

Comerón, F. & Pasquali, A. 2007, A&A, 467, L23

Cox, N.L.J., Kerschbaum, F., van Marle, A.J., et al. 2012, A&A, 543,1

del Valle, M.V. & Romero, G.E. 2012, A&A, 543, 56

Egan, M.P., Price, S.D., Kraemer, K.E. 2003, AAS, 203, 5708

Gustafsson, M., Ravkilde, T., Kristensen, et al. 2010, A&A 513, 5

Hoogerwerf, R., de Bruijne, J.H.J, de Zeeuw, P.T. 2000, ApJ, 544, L133

Kaper, L., Van Loon, J.Th., Augusteijn, T. et al. 1997, ApJ, 479, L153

Kobulnicky, H.A., Gilbert, I.J., Kiminki, D.C. 2010, ApJ, 710, 549

Longair, M. 1997, "High Energy Astrophysics", Cambridge University Press

Noriega-Crespo, A., Van Buren, D., Dgani, R. 1997, AJ, 113, 780

Perets, H.B. & Subr, L. 2012, ApJ, 751, 133

Peri, C.S., Benaglia, P., Brookes, D.P., et al. 2012, A&A, 538, 108

Prinja, R.K. & Massa, D.L. 2010, A&A, 521, 55

Silva, M.D.V. & Napiwotzki, R. 2013, MNRAS, in press

Stone, R.C. 1979, ApJ, 232, 520

Tetzlaff, N., Neuhäuser, R., Hohle, M.M. 2010, MNRAS 410, 190

Wright, E.L., Eisenhardt, P.R.M., Mainzer, A.K. et al. 2010, AJ, 140, 6, 1868

Zwicky, F. 1957, *Morphological Astronomy*, SpringerVerlag, Berlin